Optical Spectroscopic Studies of Mononitrated Benzo[a]pyrenes

5 **AUTHORS**, INCLUDING:

Shubham Vyas
Colorado School of Mines

40 PUBLICATIONS **434** CITATIONS

SEE PROFILE

Kefa Onchoke
Stephen F. Austin State University

15 PUBLICATIONS **105** CITATIONS

SEE PROFILE

Optical Spectroscopic Studies of Mononitrated Benzo[a]pyrenes[†]

Shubham Vyas,[‡] Kefa K. Onchoke,[§] Cheruvallil S. Rajesh,[‡] Christopher M. Hadad,*,[‡] and Prabir K. Dutta*,[‡]

Department of Chemistry, The Ohio State University, 100 West 18th Avenue, Columbus, Ohio 43210, and Department of Chemistry, Stephen F. Austin State University, Box 13006 - SFA Station, Nacogdoches, Texas 75962-3006

Received: May 6, 2009; Revised Manuscript Received: June 30, 2009

Spectroscopic properties, including absorption, emission spectra, and excited-state lifetimes of the mononitrated benzo[a]pyrenes (NBaPs), specifically 1-, 3-, and 6-nitrobenzo[a]pyrenes (1-, 3-, and 6-NBaP), are reported, and correlations with structure are developed. With 1- and 3-NBaP, bathochromic shifts are observed in the absorption spectra. The quantum yields of emission display the following trend: BaP ≫ 6-NBaP > 1-NBaP ≈ 3-NBaP. Fluorescence lifetimes for nitrated BaPs were ∼6 to 7 times shorter than that of BaP. With the help of time-dependent density functional theory (TD-DFT), assignments of the electronic transitions are proposed and are in good agreement with the electronic spectra for the NBaPs in methanol. On the basis of optimization of the triplet states, different photochemical consequences are discussed, and the observed fluorescence quenching is explained. Changes in the electron density distributions in the ground and excited states calculated at the second-order coupled-cluster level using the resolution-of-the-identity approximation (RI-CC2) provide information about the possible mechanism of photochemical reactions of NBaPs. Correlations between the orientation of the nitro group relative to the aromatic plane and the observed properties of the NBaP are discussed.

1. Introduction

Emitted particulate matter from combustion processes, including vehicles and power plants, contain a plethora of organic compounds. Significantly, polycyclic aromatic hydrocarbons (including nitro-PAHs and oxy-PAHs) comprise ∼50−74% of mass composition.[1] Studies have shown nitro-PAHs to be cancer-enhancing and mutagenic in both human and experimental cells, and it is estimated that mono- and dinitrated PAHs account for over 50% of the total vapor- and particle-phase direct mutagenicity of ambient air.[2] The biological effects of nitro-PAHs and their photochemistry have been correlated with the nonplanarity of the structures, in particular, the orientation of the nitro group relative to the aromatic plane.[3−5]

The optical spectroscopic properties of PAHs, including assignment of the electronic transitions, have been reported.[6−9] Studies on nitro-PAHs are, however, scarce. Despite the synthesis and acquisition of electronic spectra of nitro-PAHs,[10−14] only a few studies have focused on quantitative assignments.[15] It has been observed that the substitution of a nitro group on the parent PAH causes red shifts in the absorption wavelengths.[16,17] The fluorescence spectra of NPAHs has been acquired at low temperatures[18] or via reduction of the nitro group to the correspondingly more fluorescent amino-PAH.[2,19−24] Low quantum yields of emission arise because of the quenching ability of the nitro group.

In this study, we focus on mononitrated benzo[a]pyrenes (NBaPs), namely, 1-, 3-, and 6-nitrobenzo[a]pyrenes (1-, 3-, and 6-NBaP) shown in Figure 1 and have examined the absorption and fluorescence spectra as well as their excited-
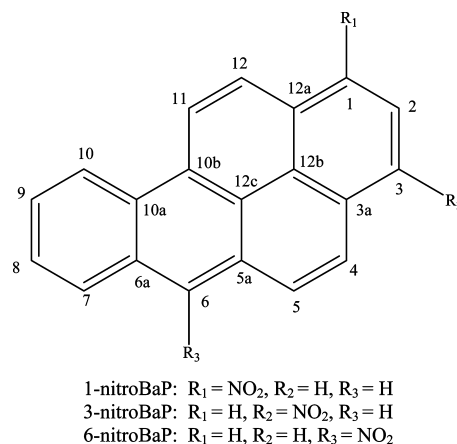

1-nitroBaP: $R_1 = NO_2$, $R_2 = H$, $R_3 = H$
3-nitroBaP: $R_1 = H$, $R_2 = NO_2$, $R_3 = H$
6-nitroBaP: $R_1 = H$, $R_2 = H$, $R_3 = NO_2$

Figure 1. General numbering system used for 1-, 3-, and 6-nitrobenzo[a]pyrene in the text.

state lifetimes at room temperature. Using time-dependent density functional theory (TD-DFT)[25,26] calculations, we have investigated the electronic structures of the ground and singlet excited states for the nitrated BaPs. We also performed electronic difference density calculations using the RI-CC2 methodology to obtain insight into the excited-state structures and known photochemistry. Furthermore, the lowest triplet states were also optimized to explain the emission spectra of these nitroaromatic compounds. Correlations are proposed between the nitro group orientation and the corresponding spectroscopic and photochemical properties.

2. Experimental Procedures

Warning! Mono-nitrobenzo[a]pyrenes (N-BaP) and their derivatives are known carcinogens and therefore should be handled with care!

Optical Spectroscopic Studies of NBaPs

J. Phys. Chem. A, Vol. 113, No. 45, 2009 **12559**

2.1. Reagents and Materials. Methanol (spectrophotometric grade, Burdick & Jackson, MI) was used. Benzo[a]pyrene (97% purity) was purchased from Aldrich. All other reagents were of analytical grade. Mononitrated benzo[a]pyrenes were synthesized and confirmed to be of high purity.

2.2. Synthesis. The synthesis of 1-, 3-, and 6-NBaP has been described elsewhere.[5] The separation of 1- and 3-NBaP (with very close dipole moments, calculated to be 6.4 and 6.5 D, respectively) was achieved via medium-pressure liquid chromatography (MPLC). ^{1}H and ^{13}C NMR spectroscopy were recorded with a 500 MHz spectrometer in $CDCl_3$.

2.3. Instrumentation/Spectroscopic Studies. Absorption and emission measurements in methanol were acquired in 1 cm path quartz cuvettes at room temperature. Absorption spectra were recorded with a UV-2501PC spectrophotometer (Shimadzu, Columbia, MD) from 200 to 600 nm. Fluorescence (excitation and emission) measurements were acquired on a SPEX Fluorolog-2 fluorimeter equipped with a Hamamatsu R928 photomultiplier. Measurements were done on degassed samples contained in sealed quartz cuvettes. The total concentration was ~0.10 absorbance units at a wavelength of 300 nm in 1 cm quartz cuvettes.

An Oxford DN1704 liquid nitrogen cryostat with ITC 502 intelligent temperature controller placed inside the Shimadzu UV/vis spectrometer was used for low-temperature experiments. The spectra were recorded in petroleum ether glass obtained by cooling the solution of NBaP to liquid-nitrogen temperature. Some amount of baseline drift was observed because of moisture condensation, even though the Oxford system is designed to minimize this effect. The temperature of the measurement chamber was under constant observation using the built-in measurement facility of the setup.

Fluorescence decay profiles of argon degassed samples (~20 min) were recorded using a time-correlated single photon counting (TCSPC) instrument. Decays were monitored at the emission maximum of the corresponding NBaPs.

The fluorescence quantum yields (Φ_f) of the NBaPs were determined by a comparative method, using recrystallized BaP in MeOH ($\Phi_f = 0.42$)[27,28] as a reference standard. The equation

$$\Phi_u = \left[\left(\frac{A_s F_u n^2}{A_u F_s n_o^2}\right)\right]\Phi_s$$

where the subscripts u and s represent the unknown and standard, respectively, Φ is the quantum yield, A is absorbance at the excitation wavelength, F is the integrated emission area across the band, and n and n_o are the index of refraction of the methanol containing the unknown (n) and the standard (n_o) at a specified temperature and at the sodium D line,[29] was used for calculating the quantum yield of the NBaPs.

2.4. Computational Details. All of the density functional theory (DFT) calculations were performed with the Gaussian 03 package[30b] of programs at the Ohio Supercomputer Center. The geometries of all structures were fully optimized at the Becke three-parameter[31,32] hybrid exchange functional combined with the Lee–Yang–Parr[33] correlation functional (B3LYP), along with the standard 6-31G* and 6-311+G** basis sets,[34] and the structures have been previously reported.[5] In all computations, no symmetry constraints were imposed on the geometry. We adopted the geometries from our earlier reports,[5] and 20 to 30 singlet states were computed for the vertical excitation energies and oscillator strengths of each NBaP at the TD-B3LYP/6-311G** level of theory. It has been shown that
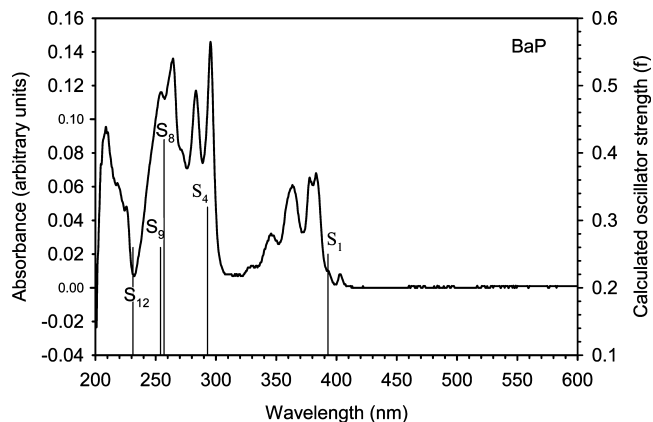

Figure 2. Experimental and calculated UV−vis absorption spectra of benzo[a]pyrene (BaP). Theoretical predictions (vertical excitation energies and oscillator strengths) made with time-dependent DFT calculations (TD-B3LYP/6-311G**) are shown as vertical bars.

the TD-B3LYP/6-311G** level of theory generally reproduces the experimental vertical excitation energies of closed- and open-shell PAHs within 0.3 eV.[35]

To gain insight into the mechanism of the photochemistry of NBaPs, electronic difference density calculations were performed for the vertical excitations of the S_1 and S_2 states on previously optimized geometries[5] at the TD-B3LYP and RI-CC2[36] level of theory with triple-ζ valence polarized (TZVP) basis sets, as employed in the Turbomole-5.80[37,38] suite of programs. In addition, corresponding triplet states were optimized at the B3LYP/6-311+G** level of theory using the Gaussian 03 suite of programs. Because attempts to obtain the difference density plots with the TD-B3LYP method failed (because of instabilities with regard to calculating the gradient on the excited-state surface), only RI-CC2 difference density plots are discussed. Occupied and unoccupied orbitals, which are involved in the vertical excitations for the S_n ($n = 1$ to 4) states, compare well between the Gaussian 03 and Turbomole packages, and hence the same singlet states are under study. (See Table S1 of the Supporting Information.) The orbitals involved and the contributions of each orbital-to-orbital configuration to each electronic transition are provided in Tables S2−S5 of the Supporting Information.

3. Results and Discussion

3.1. Absorption Spectra. Figure 1 represents the labeling used for the nitro-BaPs. The absorption spectra of BaP and the three nitro derivatives, as shown in Figures 2 and 3, are in agreement with literature.[16,39] The calculated (TD-B3LYP/6-311G**) energies and the corresponding oscillator strengths of the electronic transitions are presented graphically in Figures 2 and 3, overlaid on the observed spectra. More details of the specific nature of the transitions are shown in Tables 1−4. (Also, see Tables S2−S5 of the Supporting Information for further details). The calculations, in general, do a good job of predicting the strongest transitions. For BaP, the band predicted at 393 nm ($S_0 \rightarrow S_1$) is close to the observed value of 396 nm (Figure 2), which is in agreement with previous studies.[40] The $S_0 \rightarrow S_1$ and $S_0 \rightarrow S_2$ transitions are predominantly due to HOMO → LUMO and a combination of HOMO-1 → LUMO and HOMO → LUMO+1 transitions, respectively. Some of the less intense transitions were predicted to be under the vibronic bands; for instance, the transition to the S_5 and S_6 states in the case of BaP have very small oscillator strengths and, therefore, might be underneath the 298 nm band or its vibronic features.
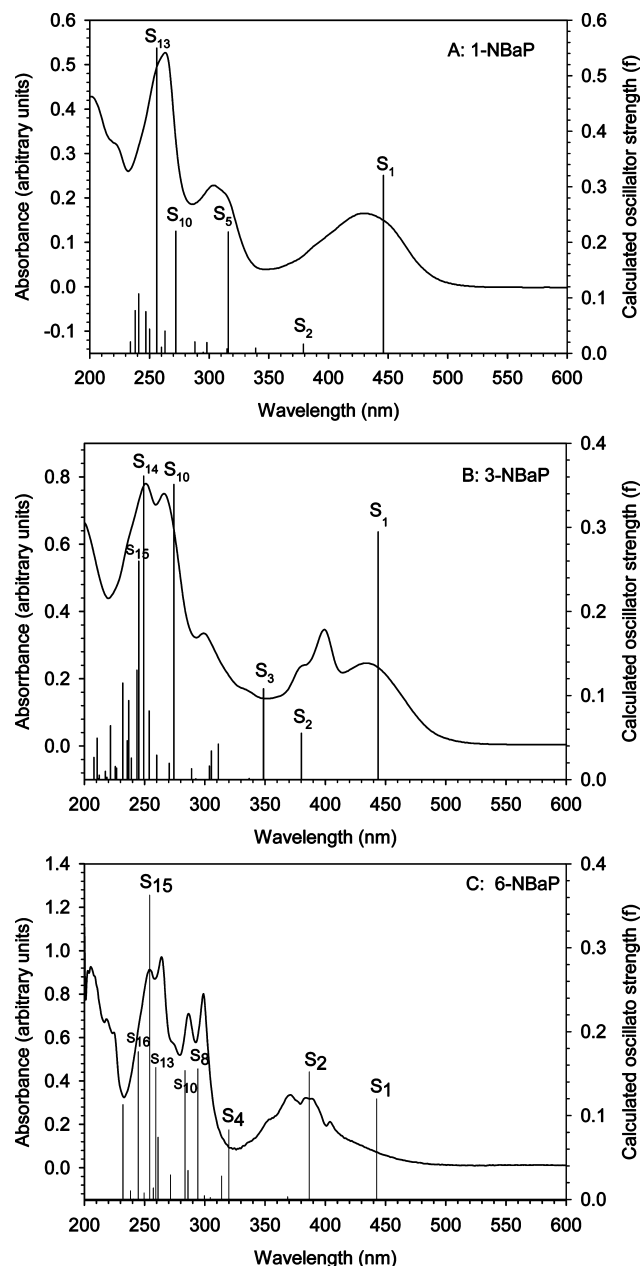
12560 *J. Phys. Chem. A, Vol. 113, No. 45, 2009*

Vyas et al.

Figure 3. Experimental and calculated UV−vis absorption spectra of (a) 1-NBaP, (b) 3-NBaP, and (c) 6-NBaP. Theoretical predictions (excitation energies and oscillator strengths) made with time-dependent DFT calculations (TD-B3LYP/6-311G**) are shown as vertical bars.

TABLE 1: Observed and Calculated Absorption Bands (nanometers), Oscillator Strengths, and Vertical Transitions in Unsubstituted Benzo[*a*]pyrene (BaP) at the TD-B3LYP/6-311G** Level of Theory[a]

state	calcd oscillator strength	calcd λ_{max} values (λ/nm)	obsd λ_{max} (nm) values (λ/nm)
S_1	0.25	393	396
S_2	0.01	362	
S_3	0.08	305	
S_4	0.32	293	298
			295
S_5	0.00	287	[b]
S_6	0.04	280	[b]
S_7	0.10	264	[b]
S_8	0.42	257	[b]
S_9	0.26	254	[b]
S_{10}	0.06	244	[b]
S_{11}	0.01	240	[b]
S_{12}	0.26	231	
S_{13}	0.05	225	225

[a] For orbital-to-orbital contributions to each vertical transition, see Table S2 of the Supporting Information. [b] Covered by the vibronic bands.

TABLE 2: Observed and Calculated Absorption Bands (nanometers), Transitions, and Oscillator Strengths in 1-Nitrobenzo[*a*]pyrene (1-NBaP) at the TD-B3LYP/6-311G** Level of Theory[a]

state	calcd oscillator strength	calcd λ_{max} values (λ/nm)	obsd λ_{max} values (λ/nm)
S_1	0.32	446	430
S_2	0.02	379	[b]
S_3	0.00	342	
S_4	0.01	339	
S_5	0.22	316	303
S_6	0.01	315	
S_7	0.02	299	
S_8	0.00	295	
S_9	0.02	288	
S_{10}	0.22	272	295
S_{11}	0.04	263	
S_{12}	0.01	260	
S_{13}	0.55	256	255

[a] For orbital-to-orbital contributions to each vertical transition, see Table S3 of the Supporting Information. [b] Covered by the vibronic bands.

For 1-NBaP (Figure 3a and Table 2), the strongest low-energy transition $S_0 \rightarrow S_1$ is predicted at 446 nm, corresponding primarily to a HOMO → LUMO transition, which is in reasonable agreement with the observed value of 430 nm. For 3-NBaP (Figure 3b and Table 3), the $S_0 \rightarrow S_1$ transition is predicted at 444 nm, as compared with the observed band at 440 nm. These transitions are assigned primarily to HOMO → LUMO transitions. For 6-NBaP (Figure 3c and Table 4), the two lowest singlet bands are calculated at 443 and 387 nm, whereas bands at 440 (shoulder) and 402 nm are observed. In contrast with the parent BaP and other nitrated structural isomers (1- and 3-NBaP), the $S_0 \rightarrow S_1$ transition of 6-NBaP is not a pure HOMO → LUMO transition and also has a significant contribution from the HOMO → LUMO+1 transition. However, the S_2 state is similar to the others, being dominated by the HOMO → LUMO+1 transition.

Figure 4 shows the MO plots corresponding to the low-energy transitions for the NBaP isomers. The MO plots were generated using the GaussView[30a] visualization software. These plots show that the LUMOs have significant involvement of the NO_2 group, whereas the HOMOs are primarily on the aromatic unit; therefore, the lowest singlet excitations can be characterized as moving electron density from the aromatic unit to the nitro group. Moreover, because the $S_0 \rightarrow S_1$ transition of 1- and 3-NBaP is largely a HOMO → LUMO transition, we expect from Figure 4 that the lowest energy transition would cause a quinoidal structure in the excited state and thus decrease the C−N bond order. However, the lowest energy transition of 6-NBaP involves considerable contribution from the HOMO → LUMO+1 transition in addition to the HOMO → LUMO transition, thus rendering 6-NBaP to be different from the other two isomers. Additionally, the second lowest transition of 6-NBaP also consists of both HOMO → LUMO and HOMO → LUMO+1 transitions, with the latter being dominant. The mixing of these two transitions in the S_1 as well as the S_2 states also imparts moderate intensity to these transitions, whereas only

Optical Spectroscopic Studies of NBaPs

J. Phys. Chem. A, Vol. 113, No. 45, 2009 **12561**

TABLE 3: Observed and Calculated Absorption Bands (nm), Transitions, and Oscillator Strengths in 3-Nitrobenzo[a]pyrene (3-NBaP) at the TD-B3LYP/6-311G** Level of Theory[a]

state	calcd oscillator strength	calcd λ_{max} values (λ/nm)	obsd λ_{max} values (λ/nm)
S_1	0.29	444	440
S_2	0.06	380	b
S_3	0.11	349	
S_4	0.00	337	
S_5	0.04	311	
S_6	0.03	305	
S_7	0.07	304	
S_8	0.00	293	
S_9	0.01	289	
S_{10}	0.35	274	265
S_{11}	0.02	270	
S_{12}	0.03	260	
S_{13}	0.08	254	
S_{14}	0.36	249	250
S_{15}	0.26	245	b
S_{16}	0.13	244	b

[a] For orbital-to-orbital contributions to each vertical transition, see Table S4 of the Supporting Information. [b] Covered by the vibronic bands.

TABLE 4: Observed and Calculated Absorption Bands (nm), Transitions, and Oscillator Strengths in 6-Nitrobenzo[a]pyrene (6-NBaP) at the TD-B3LYP/6-311G** Level of Theory[a]

state	calcd oscillator strength	calcd λ_{max} values (λ/nm)	obsd λ_{max} values (λ/nm)
S_1	0.12	443	weak shoulder at 440
S_2	0.15	387	400
S_3	0.00	369	
S_4	0.08	320	
S_5	0.03	314	
S_6	0.00	305	
S_7	0.00	300	
S_8	0.16	294	298
S_9	0.03	286	
S_{10}	0.15	284	b
S_{11}	0.03	271	
S_{12}	0.07	261	
S_{13}	0.16	260	264
S_{14}	0.014	257	
S_{15}	0.36	255	b
S_{16}	0.18	245	

[a] For orbital-to-orbital contributions to each vertical transition, see Table S5 in the Supporting Information. [b] Covered by the vibronic bands.

the S_1 state carries a high oscillator strength and with the S_2 state being a dark state for both 1- and 3-NBaP (Tables 2−4 and Figure 3).

Absorption spectra of all of these compounds were also recorded at 77 K to resolve the vibronic bands, but minimal improvement in the resolution was observed (data provided in the Supporting Information; there are a few weak peaks in all of these spectra, e.g., 510, 525, and 580 nm, which possibly arise from impurities incorporated during the chromatography).

3.2. Emission Spectra. The fluorescence spectra of BaP and 6-NBaP are shown in Figure 5. The fluorescence quantum yield (Φ_f) of 6-NBaP relative to BaP ($\Phi_f = 0.42$[27,28]) in degassed methanol is 0.03. The emission from 1-NBaP and 3-NBaP was significantly weaker than that from 6-NBaP and is considered to be nonfluorescent (Figure S5 in the Supporting Information). In the emission spectra of 6-NBaP, there is a very weak shoulder

at 417 nm, which we assign to an impurity species, and the 0−0 transition is assigned to the strong band at 436 nm. The fluorescence lifetimes (τ_f) of BaP and 6-NBaP were measured using a TCSPC instrument, and BaP showed a single exponential decay in methanol with a lifetime of 45 ns, comparable to previously reported data of 44 ns.[41] 6-NBaP exhibited a lifetime of 6.6 ns but with a second component (∼10%) with a lifetime of 3.8 ns; the latter is possibly due to an impurity.

Visualization of the total electronic redistribution after a vertical excitation was made possible via a difference density plot.[42] Such plots provide information regarding probable geometrical changes on the excited-state potential energy surfaces. Therefore, the total electron density of the ground state wave function was subtracted from the total electron density of the excited state at the S_0 geometry; the resulting difference density can then be visualized by a contouring envelope at some value of the electron density. Such an approach was recently utilized to understand the excited states of various aryl azides[43] and N-confused porphyrins.[42]

Difference density plots for the vertical S_1 and S_2 states for 1-, 3-, and 6-NBaP are shown in Figures 6 and 7. In these plots, the depletion of the electron density is shown in red, and the accumulation of electron density in the excited state upon vertical excitation is shown in green. All of the plots are shown with the same contour value. For the S_1 state of 1- and 3-NBaP, accumulation of electron density is observed at the C−N bond, which suggests a partial C−N π-bond formation in these cases. In contrast, no accumulation of electron density along the C−N bond is noted for the S_1 state of 6-NBaP, but rather accumulation of electron density in the π^* orbitals of the nitro group is observed. For the S_2 states of 1-, 3-, and 6-NBaP, accumulation of electron density in the π^* (NO_2) orbitals is evident for all of the isomers at a lower contour, as shown in Figure 7. At a higher contour value (Figure S1 in the Supporting Information), depletion of the electron density along the C-NO_2 π-bond is also noted. It is also noteworthy that 6-NBaP tends to have significantly more electron density on the aromatic system than the other structural isomers.

The geometry of the T_1 state was optimized at the UB3LYP/ 6-311+G** level of theory. These triplet geometries are shown in Figure 8. Both 1- and 3-NBaP attained completely planar geometries in the T_1 states. In 6-NBaP, the nitro group had a torsion angle of 46° in the optimized T_1 state. In addition, characteristic changes were observed in the aromatic unit making the conjugated system to be more quinoidal for all three NBaPs. The C−N bond lengths were also found to be decreased by about 0.03 Å for the optimized T_1 states when compared with the S_0 geometries.

The observed fluorescence yields and lifetimes for the NBaPs can be rationalized on the basis of the geometries of the triplet excited states and possible geometries of the lowest singlet excited state; specifically, one can speculate that if these geometries are similar, then intersystem crossing (ISC) will be more facile. The planar triplet structure for 1- and 3-NBaP is similar to the S_1 excited-state geometries due to π-bonding at the C−N moiety, and thus the singlet excited state has an additional path of decay other than just internal conversion (IC) to the ground state. The ISC would be less allowed for the S_1 state of 6-NBaP because of differences in the possible singlet excited-state and triplet-state geometry, resulting in the observed higher quantum yield and lifetime for fluorescence.

3.3. Photochemistry of Mononitrated Benzo[a]pyrenes. The difference density plots shown in Figures 6 and 7 also provide insight into the reported photochemistry of nitroaro-
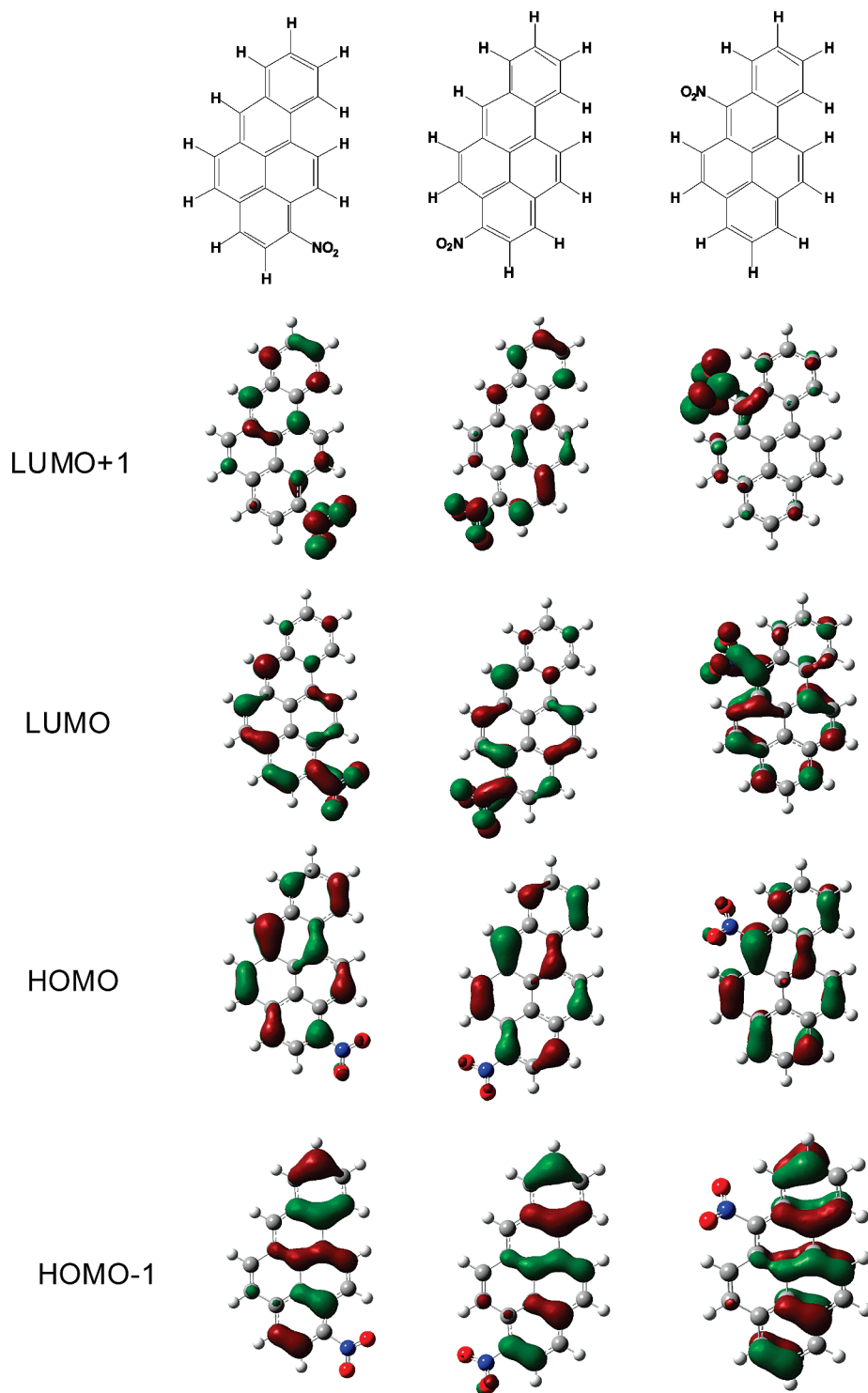
Figure 4. Occupied and unoccupied molecular orbitals (MOs) involved in the transitions for the $S_0 \rightarrow S_1$ and $S_0 \rightarrow S_2$ states for the nitrated benzo[*a*]pyrenes: (left) 1-NBaP; (center) 3-NBaP; and (right) 6-NBaP. ($S_0 \rightarrow S_1$: HOMO $\rightarrow$ LUMO; $S_0 \rightarrow S_2$: HOMO $\rightarrow$ LUMO+1, primarily. HOMO-1 is MO76, HOMO is MO77, LUMO is MO78, and LUMO+1 is MO79).

matic compounds, in general. Two mechanisms are suggested in the literature for the photochemistry of nitroaromatic compounds, namely, dissociative−associative and intramolecular rearrangement mechanisms, as shown in Figure 9.[17] The dissociative−associative mechanism involves the reversible homolytic cleavage of the C−N bond toward $NO_2^•$ and aryl radical formation, followed by the recombination of both radicals to give the corresponding aryl nitrite (Ar-ONO). Conversely, the intramolecular rearrangement mechanism depends on the rotation of the nitro group relative to the aromatic plane.[44,45] It has been proposed that if the nitro group is significantly twisted relative to the plane of the aromatic ring, then in the (n,π*) excited state, overlap may take place between the half-filled, nonbonding p orbital of the oxygen and the adjacent sp^2 orbital of the aromatic ring to form a three-membered ring, which can lead to the corresponding aryl nitrite.[17] Whereas the dissociative−associative mechanism has been observed in the case of nitromethane,[46,47] the intramolecular rearrangement mechanism has been recommended for the nitroaromatic compounds.[17] Semiempirical

Optical Spectroscopic Studies of NBaPs
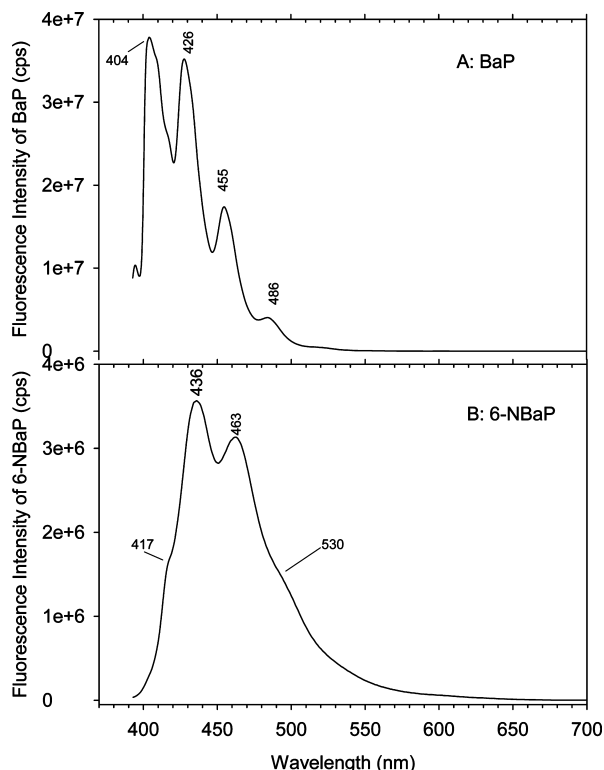
J. Phys. Chem. A, Vol. 113, No. 45, 2009 **12563**

Figure 5. Fluorescence emission spectra of (a) benzo[a]pyrene (BaP) and (b) 6-nitrobenzo[a]pyrene (6-NBaP) obtained in methanol (λ_{exc} = 383 nm, the 0−0 band of 6-NBaP is assigned to the 436 nm band).

calculations[44,45] have also been reported to corroborate the rearrangement mechanism.

There are a few studies on the photochemistry of the NBaP isomers. It has been reported that the 6-isomer decays faster under photoirradiation as compared with the 1- and 3-isomers,[48] and the intramolecular arrangement was proposed to be occurring for 6-NBaP. Also, the 6-isomer was found to release NO upon photodecomposition, whereas the 1- and 3-NBaP did not. Our calculations show no accumulation of electron density along the C−N bond for the S_1 state of 6-NBaP (Figures 6 and 7), but rather accumulation of electron density in the π^* orbitals of the nitro group is observed, suggesting that radical chemistry involving the nitro radical ($NO_2^{\bullet}$) formation is more likely for the 6-isomer (dissociative−associative mechanism). Moreover, this mechanism appears to be unlikely for 1- and 3-NBaP because of the accumulation of electron density (i.e., strengthening) of the C−N bond. However, for photochemistry mediated through the S_2 state, the dissociative−associative mechanism should be favored for all of the isomers because electron density is transferred to the π^* orbital of the nitro group and can promote $NO_2^{\bullet}$ formation.

3.4. Structural Correlations. The absorption and emission spectra, their lifetimes, and the reported photochemistry of the 6-isomer are quite distinct from the 1-and 3-NBaP isomers. Major structural differences among the three isomers are related to the orientation of the C−C−N−O dihedral angles that describe the orientation of the NO_2 group relative to the aryl plane. For the 1- and 3-NBaP isomers, calculations have shown that the dihedral angles are on the order of 29 and 30°, respectively, whereas 6-NBaP was predicted to have a C−C−N−O dihedral angle of 68°.[5] (Gas-phase and X-ray structural studies[49] support the assignment for 6-NBaP.)

Can the spectroscopic properties and the photochemistry be correlated with the orientation of the NO_2 group? For the
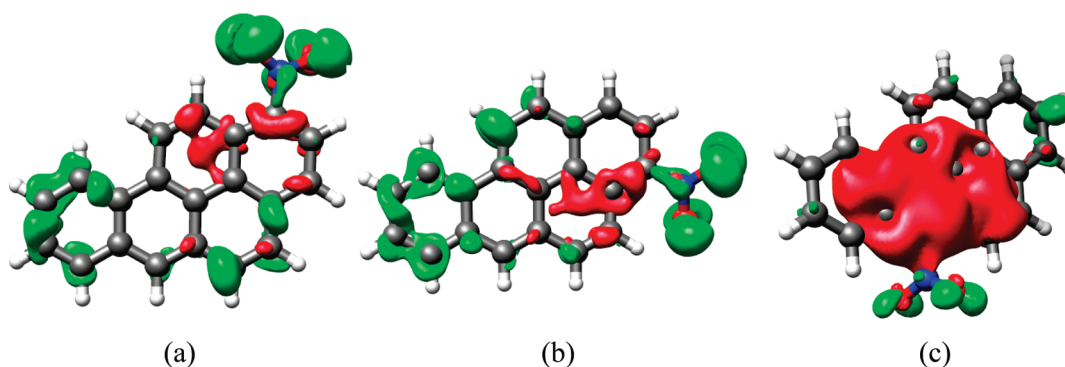

(a)   (b)   (c)

Figure 6. Vertical difference density plots at the RI-CC2/TZVP level for the S_1 state of (a) 1-NBaP, (b) 3-NBaP, and (c) 6-NBaP. The depletion of the electron density from the ground state is shown in red, and the accumulation of electron density in the S_1 excited state is shown in green (contour value is −0.01 (red) and +0.0005 (green) in au).
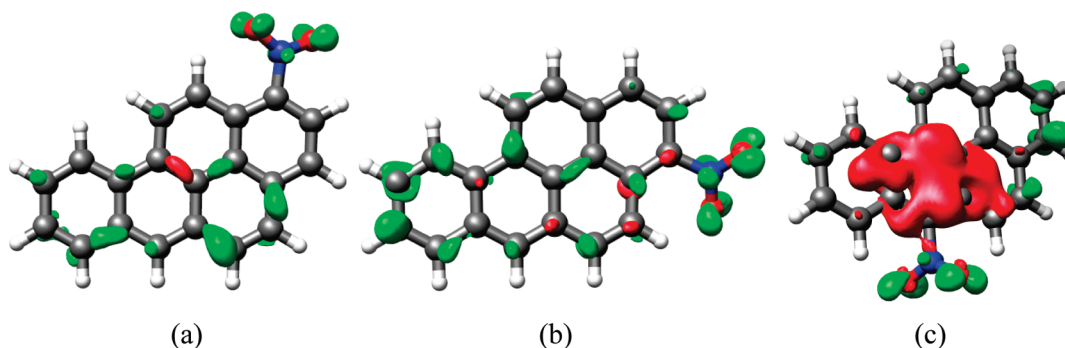

(a)   (b)   (c)

Figure 7. Vertical difference density plots at the RI-CC2/TZVP level for the S_2 state of (a) 1-NBaP, (b) 3-NBaP, and (c) 6-NBaP. The depletion of the electron density from the ground state is shown in red, and the accumulation of electron density in the S_2 excited state is shown in green (contour value is −0.01 (red) and +0.0005 (green) in au).
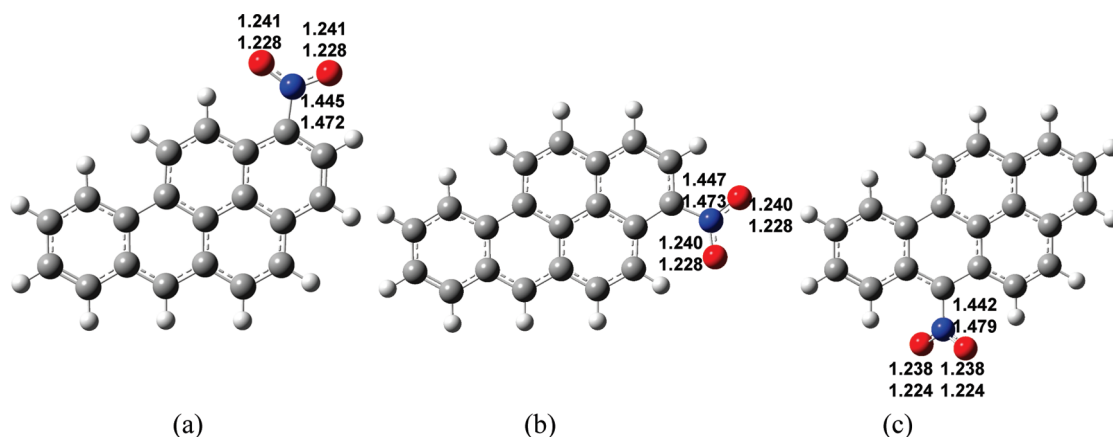
Figure 8. Optimized lowest triplet (T_1) (top number) and singlet (S_0) (bottom number) state geometries for (a) 1-NBaP, (b) 3-NBaP, and (c) 6-NBaP at UB3LYP/6-311+G** level of theory (selected bond lengths are in units of angstroms).
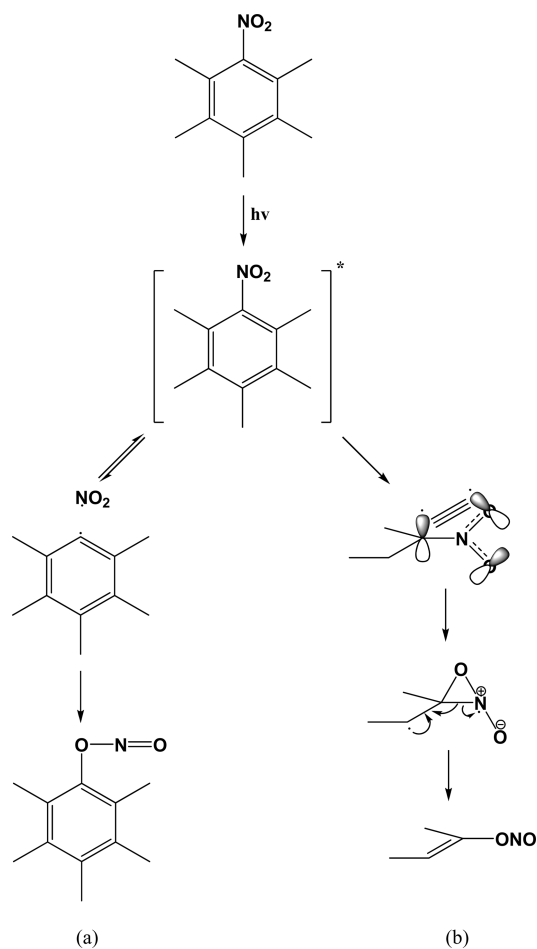

Figure 9. Proposed mechanisms for the photochemistry of nitroaromatic compounds: (a) dissociation—association mechanism[46,47] and (b) intramolecular rearrangement mechanism.[17,44,45]

absorption spectra, 1- and 3-NBaP exhibit red shifts, as compared with BaP, whereas the spectra of 6-NBaP and BaP are similar. This can be correlated to the interaction between the nitro group and BaP ring through $\pi-\pi^*$ conjugation in the 1- and 3-NBaP isomers, whereas in 6-NBaP, the two parts of the molecule are isolated, and spectroscopic properties resemble those of BaP. Our calculations indicate that in both the singlet and triplet excited states of 1- and 3-NBaP, the nitro group is coplanar with the ring, whereas in 6-NBaP, the nitro group is not. The extended conjugation between the BaP ring and the NO_2 group in 1- and 3-NBaP promotes ISC to the triplet

manifold and can explain the decreased quantum yield of fluorescence emission. The out-of-plane geometry in the excited state of 6-NBaP can also account for its different photochemistry as compared with that of the other two isomers.

5. Conclusions

For BaP with an NO_2 group at the 1- and 3-positions, strong UV—vis absorption bands are red-shifted, as compared with BaP, in their absorption spectra, whereas the red-shifted band in 6-NBaP was considerably smaller. On the basis of MO plots, the $\pi_{BaP} \rightarrow \pi^*_{BaP,NO2}$ excitations were found to be dominant in the S_1 state of 1-, 3-, and 6-NBaP. Increased orbital overlaps between the aromatic moiety and the nitro group enhanced the extent of conjugation and thus enhanced the oscillator strength of the low-energy absorption band, which is consistent with the C—C—N—O dihedral angle in the ground (S_0) state: 6-NBaP (62°) > 3-NBaP (~30°) ≈ 1-NBaP (30°). The quantum yield of emission for 6-NBaP was higher than that for 1- and 3-NBaP, suggesting that ISC is promoted by the coplanar orientations of the NO_2 and aryl units in the singlet and triplet states. Difference density plots for the S_1 excited states suggest that photochemistry via the low-lying singlet excited states should proceed through a dissociative—associative mechanism for 6-NBaP but is unlikely for the 1- and 3-NBaP isomers. However, photochemistry via the S_2 state can proceed through a dissociative—associative mechanism for all three isomers. The triplet manifold was found to have significant structural differences among 1, 3-, and 6-NBaPs. It can also be concluded that the T_1 state would not generate the aryloxy radical and nitric oxide.

Supporting Information Available: Difference density plots at RI-CC2/TZVP, low-temperature absorption spectra of NBaPs in diethyl ether glass, fluorescence emission spectra of 1- and 3-NBaP, comparison between Gaussian 03 and Turbomole 5.80 calculations, experimental and theoretical (TD-B3LYP/6-311G**) absorption bands, oscillator strengths (f), vertical excitation energies (ω), and transitions of benzo[a]pyrene and

Optical Spectroscopic Studies of NBaPs

J. Phys. Chem. A, Vol. 113, No. 45, 2009 **12565**

1-, 3-, and 6-NBaPs, optimized triplet-state geometries, and NMR data of the NBaPs. This material is available free of charge via the Internet at http://pubs.acs.org.

References and Notes

(1) Cass, G. R.; Hughes, L. A.; Bhave, P.; Kleeman, M. J.; Allen, J. A.; Salmon, L. G. *Philos. Trans. R. Soc. London, Ser. A* **2000**, *358*, 2581.

(2) Schauer, C.; Niessner, R.; Poschl, U. *Anal. Bioanal. Chem.* **2004**, *378*, 725.

(3) Fu, P. P.; Chou, M. W.; Miller, D. W.; White, G. L.; Heflich, R. H.; Beland, F. A. *Mutat. Res.* **1985**, *143*, 173.

(4) Fukuhara, K.; Takei, M.; Kageyama, H.; Miyata, N. *Chem. Res. Toxicol.* **1995**, *8*, 47.

(5) Onchoke, K. K.; Hadad, C. M.; Dutta, P. K. *J. Phys. Chem. A* **2006**, *110*, 76.

(6) Schwarz, F. P.; Wasik, S. P. *Anal. Chem.* **1976**, *48*, 524.

(7) Dabestani, R.; Ivanov, I. N. *Photochem. Photobiol.* **1999**, *70*, 10.

(8) Reyes, C. A.; Medina, M.; Crespo-Hernandez, C.; Cedeno, M. Z.; Arce, R.; Rosario, O.; Steffenson, D. M.; Ivanov, I. N.; Sigman, M. E.; Dabestani, R. *Environ. Sci. Technol.* **2000**, *34*, 415.

(9) Desilets, D. J.; Kissinger, P. T.; Lyte, F. E. *Anal. Chem.* **1987**, *59*, 1830.

(10) Mulder, P. P. J.; Boerriger, J. O.; Boere, B. B.; Zuihof, H.; Erkelens, C.; Cornelisse, J.; Lugtenburg, J. *Recl. Trav. Chim. Pays−Bas* **1993**, *112*, 287.

(11) Hansen, P. E.; Berg, A. *Acta Chem. Scand., Ser. B* **1981**, *35*, 131.

(12) van den Braken-van Leersum, A. M.; C, T.; van't Zelfde, M.; Cornelisse, J.; Lugtenburg, J. *Recl. Trav. Chim. Pays−Bas* **1987**, *106*, 120.

(13) van den Braken-van Leersum, A. M.; Spijker, N. M.; Lugtenburg, J.; Cornelisse, J. *Recl. Trav. Chim. Pays−Bas* **1987**, *106*, 628.

(14) Goldring, J. M.; Ball, L. M.; Sangaiah, R.; Gold, A. *EPA* **1986**, *EPA/600/D-86/182*, 1.

(15) Hamanoue, K.; Nakayama, T.; Kajiwara, K.; Yamanaka, S. *J. Chem. Soc., Faraday Trans.* **1992**, *88*, 3145.

(16) Chou, M. W.; Heflich, R. H.; Casciano, D. A.; Miller, D. W.; Freeman, J. E.; Evans, F. E.; Fu, P. P. *J. Med. Chem.* **1984**, *27*, 1156.

(17) Chapman, O. L.; Heckert, D. C.; Reasoner, J. W.; Thackaberry, S. P. *J. Am. Chem. Soc.* **1966**, *88*, 5550.

(18) Matsuzawa, S.; Garrigues, P.; Budzinski, H.; Bellocq, J.; Shimizu, Y. *Anal. Chim. Acta* **1995**, *312*, 165.

(19) Kuo, C.-T.; Chen, H.-W.; Lin, S.-T. *Anal. Chim. Acta* **2003**, *482*, 219.

(20) Tejada, S. B.; Zweidinger, R. B.; Sigsby, J. E., Jr. *Anal. Chem.* **1986**, *58*, 1827.

(21) Campbell, R. M.; Lee, M. L. *Anal. Chem.* **1984**, *56*, 1026.

(22) Jinhui, X.; Lee, F. S. C. *Anal. Chim. Acta* **2000**, *416*, 111.

(23) Robbat, A., Jr.; Corso, N. P.; Doherty, P. J.; Wolf, M. H. *Anal. Chem.* **1986**, *58*, 2078.

(24) Murayama, M.; Dasgupta, P. K. *Anal. Chem.* **1996**, *68*, 1226.

(25) Furche, F.; Ahlrichs, R. J. *J. Chem. Phys.* **2002**, *117*, 7433.

(26) Furche, F.; Ahlrichs, R. J. *J. Chem. Phys.* **2004**, *121*, 12772.

(27) Parker, C. A.; Hatchard, C. G.; Joyce, T. A. *J. Mol. Spectrosc.* **1964**, *14*, 311.

(28) Murov, S. L.; Hug, G. L.; Carmichael, I. *Handbook of Photochemistry*, 2nd ed.; Marcel Dekker: New York, 1993.

(29) Eaton, D. F. Luminescence Spectroscopy. In *CRC Handbook of Organic Photochemistry*; Scaiano, J. C., Ed.; CRC Press: Boca Raton, FL, 1987; Vol. 1, pp 231.

(30) (a) Dennington, R., III; Keith, T.; Millam, J.; Eppinnett, K.; Hovell, W. L.; Gilliland, R. *GaussView*, version 4.1; Semichem, Inc.: Shawnee Mission, KS, 2003. (b) Frisch, M. J.; Trucks, G. W.; Schlegel, H. B.; Scuseria, G. E.; Robb, M. A.; Cheeseman, J. R.; Montgomery, J. A., Jr.; Vreven, T.; Kudin, K. N.; Burant, J. C.; Millam, J. M.; Iyengar, S. S.; Tomasi, J.; Barone, V.; Mennucci, B.; Cossi, M.; Scalmani, G.; Rega, N.; Petersson, G. A.; Nakatsuji, H.; Hada, M.; Ehara, M.; Toyota, K.; Fukuda, R.; Hasegawa, J.; Ishida, M.; Nakajima, T.; Honda, Y.; Kitao, O.; Nakai, H.; Klene, M.; Li, X.; Knox, J. E.; Hratchian, H. P.; Cross, J. B.; Bakken, V.; Adamo, C.; Jaramillo, J.; Gomperts, R.; Stratmann, R. E.; Yazyev, O.; Austin, A. J.; Cammi, R.; Pomelli, C.; Ochterski, J. W.; Ayala, P. Y.; Morokuma, K.; Voth, G. A.; Salvador, P.; Dannenberg, J. J.; Zakrzewski, V. G.; Dapprich, S.; Daniels, A. D.; Strain, M. C.; Farkas, O.; Malick, D. K.; Rabuck, A. D.; Raghavachari, K.; Foresman, J. B.; Ortiz, J. V.; Cui, Q.; Baboul, A. G.; Clifford, S.; Cioslowski, J.; Stefanov, B. B.; Liu, G.; Liashenko, A.; Piskorz, P.; Komaromi, I.; Martin, R. L.; Fox, D. J.; Keith, T.; Al-Laham, M. A.; Peng, C. Y.; Nanayakkara, A.; Challacombe, M.; Gill, P. M. W.; Johnson, B.; Chen, W.; Wong, M. W.; Gonzalez, C.; Pople, J. A. *Gaussian 03*, revision C.02; Gaussian, Inc.: Wallingford, CT, 2004.

(31) Becke, A. D. *J. Chem. Phys.* **1983**, *98*, 5643.

(32) Becke, A. D. *Phys. Rev. A* **1988**, *38*, 3098.

(33) Lee, C.; Yang, W.; Parr, R. G. *Phys. Rev. B* **1988**, *37*, 785.

(34) Hariharan, P. C.; Pople, J. A. *Theor. Chim. Acta* **1973**, *28*, 213.

(35) Wang, H.; Szcepanski, J.; Hirata, S.; Vala, M. *J. Phys. Chem. A* **2005**, *109*, 9737.

(36) Hättig, C.; Weigend, F. *J. Chem. Phys.* **2000**, *113*, 5154.

(37) Ahlrichs, R.; Bär, M.; Häser, M.; Horn, H.; Kölmel, C. *Chem. Phys. Lett.* **1989**, *162*, 165.

(38) Treutler, O.; Ahlrichs, R. *J. Chem. Phys.* **1995**, *102*, 346.

(39) Fioressi, S.; Arce, R. *J. Phys. Chem. B* **2003**, *107*, 5968.

(40) Gittins, C. M.; Rohlfing, E. A.; Rohlfing, C. M. *J. Chem. Phys.* **1996**, *105*, 7323.

(41) Imasaka, T.; Kawabata, Y.; Ishibashi, N. *Rev. Sci. Instrum.* **1981**, *52*, 1473.

(42) Vyas, S.; Hadad, C. M.; Modarelli, D. A. *J. Phys. Chem. A* **2008**, *112*, 6533–6549.

(43) (a) Burdzinski, G. T.; Gustafson, T. L.; Hackett, J. C.; Hadad, C. M.; Platz, M. S. *J. Am. Chem. Soc.* **2005**, *127*, 13764. (b) Burdzinski, G.; Hackett, J. C.; Wang, J.; Gustafson, T. L.; Hadad, C. M.; Platz, M. S. *J. Am. Chem. Soc.* **2006**, *128*, 13402. (c) Wang, J.; Kubicki, J.; Burdzinski, G.; Hackett, J. C.; Gustafson, T. L.; Hadad, C. M.; Platz, M. S. *J. Org. Chem.* **2007**, *72*, 7581.

(44) Fukuhara, K.; Kurihara, M.; Miyata, N. *J. Am. Chem. Soc.* **2001**, *123*, 8662.

(45) Warner, S. D.; Farrant, J.-P.; Butler, I. S. *Chemosphere* **2004**, *54*, 1207.

(46) Brown, H. W.; Pimentel, G. C. *J. Chem. Phys.* **1958**, *29*, 883.

(47) Rebbert, R. E.; Slagg, W. *Bull. Soc. Chim. Belg.* **1962**, *71*, 708.

(48) Ishii, S.; Hisamatsu, Y.; Inazu, K.; Kobayashi, T.; Aika, K. *Chemosphere* **2000**, *41*, 1809–1819.

(49) Warner, S. D.; Lebuis, A.-M.; Farant, J.-P.; Butler, I. S. *J. Chem. Crystallogr.* **2003**, *33*, 213.